



Thermal entanglement and thermal discord in two-qubit Heisenberg XYZ chain with Dzyaloshinskii–Moriya interactions

DaeKil Park^{1,2}

Received: 21 January 2019 / Accepted: 16 April 2019
© Springer Science+Business Media, LLC, part of Springer Nature 2019

Abstract

In order to explore the effect of external temperature T in quantum correlation, we compute thermal entanglement and thermal discord analytically in the Heisenberg $X Y Z$ model with Dzyaloshinskii–Moriya interaction term $\mathbf{D} \cdot (\sigma_1 \times \sigma_2)$. For the case of thermal entanglement, it is shown that quantum phase transition occurs at $T = T_c$ due to sudden death phenomenon. For antiferromagnetic case, the critical temperature T_c increases with increasing $|\mathbf{D}|$. For ferromagnetic case, however, T_c exhibits different behavior in the regions $|\mathbf{D}| \geq |\mathbf{D}_*|$ and $|\mathbf{D}| < |\mathbf{D}_*|$, where \mathbf{D}_* is particular value of \mathbf{D} . It is shown that T_c becomes zero at $|\mathbf{D}| = |\mathbf{D}_*|$. We explore the behavior of thermal discord in detail at $T \approx T_c$. For antiferromagnetic case, the external temperature makes the thermal discord exhibit exponential damping behavior, but it never reaches exact zero. For ferromagnetic case, the thermal entanglement and thermal discord are shown to be zero simultaneously at $T_c = 0$ and $|\mathbf{D}| = |\mathbf{D}_*|$. This is unique condition for simultaneous disappearance of thermal entanglement and thermal discord in this model.

Keywords Thermal entanglement · Thermal discord · Dzyaloshinskii–Moriya interactions

1 Introduction

Recently, much attention has been paid to quantum technology developed on the foundation of quantum information processing (QIP). The physical resource of QIP is quantum correlation such as quantum entanglement [1–3] and quantum discord [4,5].

✉ DaeKil Park
dkpark@kyungnam.ac.kr

¹ Department of Electronic Engineering, Kyungnam University, Changwon 631-701, Korea

² Department of Physics, Kyungnam University, Changwon 631-701, Korea

Thus, they are at the heart in various QIP such as quantum teleportation [6], superdense coding [7], quantum cloning [8], quantum cryptography [9,10], quantum metrology [11], and quantum computer [12,13]. In particular, physical realization of quantum cryptography and quantum computer seems to be accomplished in the near future.¹

Pure quantum mechanical phenomena can occur in ideally closed system. However, real physical systems inevitably interact with their surroundings. Then, quantum systems undergo decoherence [15] and, as a result, lose their quantum properties. Thus, the environment can make various QIP useless due to disappearance of quantum correlation. In order to develop the quantum technology, therefore, it is important to study effect of its surroundings precisely.

Usually, decoherence significantly changes the quantum correlation. For example, decoherence makes degradation of entanglement and discord. For the case of entanglement, the entanglement sudden death (ESD) occurs sometimes when the entangled multipartite quantum system is embedded in Markovian environments [16–20]. This means that the entanglement is completely disentangled at finite times. Most typical environment is external temperature. If external temperature induces the ESD phenomenon in a system, this implies that quantum phase transition occurs at critical temperature T_c . This means that quantum entanglement completely disappears at $T \geq T_c$. The purpose of this paper is to examine how quantum entanglement and quantum discord are degraded due to external temperature and to study on the quantum phase transition in detail by introducing the anisotropic Heisenberg $X Y Z$ chain system with Dzyaloshinskii–Moriya (DM) interaction [21,22]. The quantum phase transition of a spin-3 Heisenberg model with DM interaction was discussed in Ref. [23].

Heisenberg model is a simple spin chain model, which is used to simulate many physical systems such as nuclear spins [24], quantum dots [25–27], superconductor [28,29], and optical lattices [30]. Since spin is two-level, Heisenberg model is ideal for generation of qubit states. Thus, this model attracts attention recently for realization of solid-based quantum computer. In Ref. [31], the DM interaction terms are introduced in this model due to spin–orbit couplings. The general Hamiltonian for N -spin Heisenberg model with DM interaction is

$$H_N = \sum_{i=1}^{N-1} [J_x \sigma_i^x \otimes \sigma_{i+1}^x + J_y \sigma_i^y \otimes \sigma_{i+1}^y + J_z \sigma_i^z \otimes \sigma_{i+1}^z + \mathbf{D} \cdot (\boldsymbol{\sigma}_i \times \boldsymbol{\sigma}_{i+1})], \quad (1.1)$$

where the last term is called the DM interaction arising from spin–orbit couplings.² The real parameters J_α ($\alpha = x, y, z$) denote the symmetric exchange spin–spin interactions, \mathbf{D} is the antisymmetric DM exchange interaction, and $\sigma_i^{x,y,z}$ are Pauli spin operators on the site i . The negative and positive J_α ($\alpha = x, y, z$) correspond to the ferromagnetic and antiferromagnetic nature of the system, respectively. If $J_x = J_y \neq J_z$, this system is called $X X Z$ model with DM interaction.

¹ See Ref. [14] and web page <https://www.computing.co.uk/ctg/news/3065541/european-union-reveals-test-projects-for-first-tranche-of-eur1bn-quantum-computing-fund>.

² In addition to DM interaction, the spin–orbit coupling induces the second-order term called Γ tensor [32–34]. This term is neglected in this paper. This means that our paper is valid only in the first-order correction of spin–orbit interaction.

In this paper, we study on the effect of external temperature in the entanglement and discord based on the analytic results by introducing 2-qubit Heisenberg model with DM interaction. In particular, we focus on the quantum phase transition in entanglement, which occurs due to ESD phenomena. Our motivation is as follows. Although definitions of entanglement and discord are completely different, these are two different measures of quantum correlation. Thus, we guess they should exhibit similar behavior to each other. In order to confirm our conjecture, we examine in detail the behavior of thermal discord at $T \approx T_c$. It is shown that for antiferromagnetic case ($J_\alpha > 0$) the temperature dependence of discord exhibits an exponential damping behavior, but it never reaches zero. This means that thermal discord does not completely vanish in the separable states arising from thermal density matrix at $T \geq T_c$. For ferromagnetic case ($J_\alpha < 0$), it is shown that the critical temperature T_c approaches zero if the DM coupling constant \mathbf{D} approaches a particular value \mathbf{D}_* . At $\mathbf{D} = \mathbf{D}_*$, thermal discord completely vanishes at $T = T_c = 0$. The point $\mathbf{D} = \mathbf{D}_*$ and $T = 0$ in parameter space is a unique point, where the thermal entanglement and thermal discord simultaneously vanish.

The paper is organized as follows. In Sect. 2, we derive the thermal density matrices $\rho_Z(T)$ when $D_x = D_y = 0$ and $\rho_Y(T)$ when $D_x = D_z = 0$. The case of $D_y = D_z = 0$ is not presented in this paper because all calculation is very similar to the case of $D_x = D_z = 0$. If two components of \mathbf{D} are nonzero, we should rely on numerical analysis for computation of entanglement and discord. Thus, these cases are not considered in this paper. In Sect. 3, we compute the thermal entanglement of $\rho_Z(T)$ and $\rho_Y(T)$ analytically. Using our analytical results, we examine the critical temperature T_c , above which the thermal entanglement completely vanishes. It is shown that for antiferromagnetic case ($J_\alpha > 0$, $\alpha = x, y, z$) the critical temperature is determined by single equation for each thermal density matrix. For ferromagnetic case ($J_\alpha < 0$, $\alpha = x, y, z$), however, the critical temperature is determined by two different equations in the two separate two regions $|\mathbf{D}| \geq |\mathbf{D}_*|$ and $|\mathbf{D}| < |\mathbf{D}_*|$. It is shown that T_c becomes zero at the boundary of these region $|\mathbf{D}| = |\mathbf{D}_*|$. In Sect. 4, the thermal discords of $\rho_Z(T)$ and $\rho_Y(T)$ are analytically computed. Using the analytic results, we examine the behavior of thermal discords near the critical temperature in detail. For antiferromagnetic case, the T -dependence of the discords exhibits exponential damping behavior with increasing T like thermal entanglement, but it does not reach exact zero. For ferromagnetic case, however, thermal discord becomes exact zero at the point $\mathbf{D} = \mathbf{D}_*$ and $T_c = 0$. The behavior of thermal discord at $T = T_c$ for arbitrary $|\mathbf{D}|$ is also examined in detail. In Sect. 5, a brief conclusion is given. In ‘‘Appendix A,’’ the thermal discord for $\rho_Y(T)$ is explicitly computed. In ‘‘Appendix B,’’ we discuss the critical behavior of concurrence when $D_x \neq 0$ and $D_y \neq 0$ for completeness.

2 Thermal density matrix

The Hamiltonian for two-spin anisotropic Heisenberg $X Y Z$ chain with DM interaction is given by [31]

$$H = J_x \sigma_1^x \otimes \sigma_2^x + J_y \sigma_1^y \otimes \sigma_2^y + J_z \sigma_1^z \otimes \sigma_2^z + \mathbf{D} \cdot (\boldsymbol{\sigma}_1 \times \boldsymbol{\sigma}_2). \quad (2.1)$$

Table 1 Eigenvalues and eigenvectors of H_Z

Eigenvalues of H_Z	Corresponding eigenvectors
$E_{1,z} = J_x - J_y + J_z$	$ z_1\rangle = \frac{1}{\sqrt{2}} (00\rangle + 11\rangle)$
$E_{2,z} = -J_x + J_y + J_z$	$ z_2\rangle = \frac{1}{\sqrt{2}} (00\rangle - 11\rangle)$
$E_{3,z} = -J_z + \xi$	$ z_3\rangle = \frac{1}{\sqrt{2}} (01\rangle + e^{i\theta} 10\rangle)$
$E_{4,z} = -J_z - \xi$	$ z_4\rangle = \frac{1}{\sqrt{2}} (01\rangle - e^{i\theta} 10\rangle)$

In Refs. [35–37], the entanglement of this model with $J_x = J_y = J_z$ and $J_x = J_y \neq J_z$ was discussed, respectively. The quantum phase transition with an applied magnetic field was studied in Ref. [38]. Also, the thermal entanglement of three-qubit ground state was discussed [39,40]. Quantum discord [4,5], another measure of quantum correlation, of this model was discussed in Ref. [41,42] when $J_x = J_y$ and in Ref. [43] when $J_z = 0$. Recently, the quantum-memory-assisted entropic uncertainties [44,45] were examined in this Heisenberg model [46].

2.1 $D_x = D_y = 0$ case

In this case, the matrix representation of the Hamiltonian in the computational basis $\{|00\rangle, |01\rangle, |10\rangle, |11\rangle\}$ becomes

$$H_Z = \begin{pmatrix} J_z & 0 & 0 & J_x - J_y \\ 0 & -J_z & J_x + J_y + 2iD_z & 0 \\ 0 & J_x + J_y - 2iD_z & -J_z & 0 \\ J_x - J_y & 0 & 0 & J_z \end{pmatrix}. \tag{2.2}$$

The eigenvalues and corresponding eigenvectors of H_Z are summarized in Table 1. In this table, ξ and θ are given by

$$\xi = \sqrt{4D_z^2 + (J_x + J_y)^2} \quad \theta = \tan^{-1} \left(-\frac{2D_z}{J_x + J_y} \right). \tag{2.3}$$

Thus, the spectral decomposition of H_Z can be written as

$$H_Z = \sum_{i=1}^4 E_{i,z} |z_i\rangle \langle z_i|. \tag{2.4}$$

The partition function of this system is given by

$$\mathcal{Z}_Z \equiv \text{Tr} \left[e^{-\beta H_Z} \right] = 2e^{-\beta J_z} \cosh [\beta (J_x - J_y)] + 2e^{\beta J_z} \cosh (\beta \xi), \tag{2.5}$$

Table 2 Eigenvalues and eigenvectors of H_Y

Eigenvalues of H_Y	Corresponding eigenvectors
$E_{1,y} = J_y + (J_x - J_z)$	$ y_1\rangle = \frac{1}{\sqrt{2}}(01\rangle + 10\rangle)$
$E_{2,y} = J_y - (J_x - J_z)$	$ y_2\rangle = \frac{1}{\sqrt{2}}(00\rangle - 11\rangle)$
$E_{3,y} = -J_y + \eta$	$ y_3\rangle = \frac{1}{\sqrt{2}}[\sin \phi_1(00\rangle + 11\rangle) - \cos \phi_1(01\rangle - 10\rangle)]$
$E_{4,y} = -J_y - \eta$	$ y_4\rangle = \frac{1}{\sqrt{2}}[\sin \phi_2(00\rangle + 11\rangle) - \cos \phi_2(01\rangle - 10\rangle)]$

where $\beta = 1/k_B T$, where k_B and T are Boltzmann constant and external temperature. Throughout this paper, we use $k_B = 1$ for convenience. Then, the thermal density matrix in this case becomes

$$\rho_Z(T) \equiv \frac{1}{\mathcal{Z}_Z} e^{-\beta H_Z} = \begin{pmatrix} r & 0 & 0 & s \\ 0 & u & v & 0 \\ 0 & v^* & u & 0 \\ s & 0 & 0 & r \end{pmatrix} \tag{2.6}$$

where

$$\begin{aligned} r &= \frac{1}{\mathcal{Z}_Z} e^{-\beta J_z} \cosh[\beta(J_x - J_y)] & s &= -\frac{1}{\mathcal{Z}_Z} e^{-\beta J_z} \sinh[\beta(J_x - J_y)] \\ u &= \frac{1}{\mathcal{Z}_Z} e^{\beta J_z} \cosh(\beta \xi) & v &= -\frac{1}{\mathcal{Z}_Z} \frac{J_x + J_y + 2iD_z}{\xi} e^{\beta J_z} \sinh(\beta \xi). \end{aligned} \tag{2.7}$$

It is worthwhile noting $r + u = 1/2$, which guarantees $\text{Tr}[\rho_Z(T)] = 1$.

The fact $\cos(\phi_1 - \phi_2) = 0$ guarantees the orthonormal condition of $|y_j\rangle$, i.e., $\langle y_i | y_j \rangle = \delta_{ij}$.

2.2 $D_x = D_z = 0$ case

In this case, the matrix representation of the Hamiltonian in the computational basis becomes

$$H_Y = \begin{pmatrix} J_z & D_y & -D_y & J_x - J_y \\ D_y & -J_z & J_x + J_y & D_y \\ -D_y & J_x + J_y & -J_z & -D_y \\ J_x - J_y & D_y & -D_y & J_z \end{pmatrix}. \tag{2.8}$$

The eigenvalues and corresponding eigenvectors of H_Y are summarized in Table 2. In this table, η , ϕ_1 , and ϕ_2 are given by

$$\begin{aligned} \eta &= \sqrt{4D_y^2 + (J_x + J_z)^2} \quad \phi_1 = \tan^{-1} \left[-\frac{2D_y}{\eta - (J_x + J_z)} \right] \\ \phi_2 &= \tan^{-1} \left[\frac{2D_y}{\eta + (J_x + J_z)} \right]. \end{aligned} \tag{2.9}$$

Thus, the spectral decomposition of H_Y is $H_Y = \sum_{i=1}^4 E_{i,y} |y_i\rangle \langle y_i|$ and the partition function is

$$\mathcal{Z}_Y \equiv \text{Tr} \left[e^{-\beta H_Y} \right] = 2e^{-\beta J_y} \cosh [\beta(J_x - J_z)] + 2e^{\beta J_y} \cosh(\beta \eta). \tag{2.10}$$

The thermal density matrix in this system can be written in a form

$$\rho_Y(T) = \frac{1}{\mathcal{Z}_Y} e^{-\beta H_Y} = \begin{pmatrix} r_1 & -q & q & r_2 \\ -q & u_1 & u_2 & -q \\ q & u_2 & u_1 & q \\ r_2 & -q & q & r_1 \end{pmatrix}, \tag{2.11}$$

where

$$\begin{aligned} r_1 &= \frac{1}{2\mathcal{Z}_Y} \left[e^{-\beta E_{2,y}} + \sin^2 \phi_1 e^{-\beta E_{3,y}} + \sin^2 \phi_2 e^{-\beta E_{4,y}} \right] \\ r_2 &= \frac{1}{2\mathcal{Z}_Y} \left[-e^{-\beta E_{2,y}} + \sin^2 \phi_1 e^{-\beta E_{3,y}} + \sin^2 \phi_2 e^{-\beta E_{4,y}} \right] \\ u_1 &= \frac{1}{2\mathcal{Z}_Y} \left[e^{-\beta E_{1,y}} + \cos^2 \phi_1 e^{-\beta E_{3,y}} + \cos^2 \phi_2 e^{-\beta E_{4,y}} \right] \\ u_2 &= \frac{1}{2\mathcal{Z}_Y} \left[e^{-\beta E_{1,y}} - \cos^2 \phi_1 e^{-\beta E_{3,y}} - \cos^2 \phi_2 e^{-\beta E_{4,y}} \right] \\ q &= \frac{1}{2\mathcal{Z}_Y} \left[\sin \phi_1 \cos \phi_1 e^{-\beta E_{3,y}} + \sin \phi_2 \cos \phi_2 e^{-\beta E_{4,y}} \right]. \end{aligned} \tag{2.12}$$

Since $r_1 + u_1 = 1/2$, it is easy to show $\text{Tr}[\rho_Y(T)] = 1$. Since $D_y = D_z = 0$ case is similar to $D_x = D_z = 0$ case, we do not explore this case in this paper.

3 Thermal entanglement

In this section, we examine the temperature dependence of entanglement for the thermal density matrices $\rho_Z(T)$ and $\rho_Y(T)$ by making use of concurrence [47,48]. Thermal entanglement of $X Y Z$ model was considered in Ref. [49] when there is no DM interaction and in Ref. [50] when one component of DM interaction is nonzero. Thus, our calculation of this section overlaps with that of Ref. [50]. However, we focus on the critical temperature T_c in detail because our main motivation is to examine the quantum discord around $T \sim T_c$. Following the procedure presented in Ref. [48], one can compute the concurrence $\mathcal{C}(\rho)$ for a quantum state ρ by a simple formula:

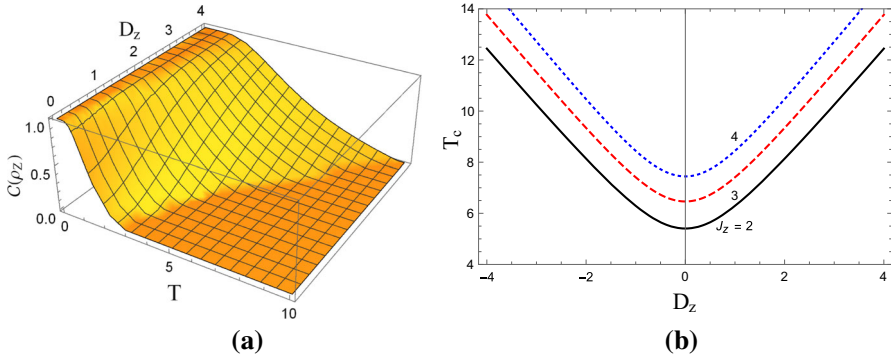


Fig. 1 (Color online) **a** The T - and D_z -dependence of concurrence $C(\rho_Z)$ in $X X Z$ model with DM interaction when $J = 1$ and $J_z = 0.2$. This figure shows that this model exhibits a quantum phase transition with the critical temperature T_c , where the entanglement completely vanishes at $T \geq T_c$. **b** The D_z -dependence of T_c when $J_z = 2$ (black line), $J_z = 3$ (red dashed line), and $J_z = 4$ (blue dotted line) with choosing $J_x = 1$ and $J_y = 1.5$. This figure shows that the critical temperature increases very rapidly with increasing $|D_z|$

$$C(\rho) = \max (\lambda_1 - \lambda_2 - \lambda_3 - \lambda_4, 0), \tag{3.1}$$

where the λ_i 's are eigenvalues, in decreasing order, of the Hermitian matrix $\sqrt{\sqrt{\rho}(\sigma_y \otimes \sigma_y)\rho^*(\sigma_y \otimes \sigma_y)\sqrt{\rho}}$.

Following this procedure, it is easy to show that the concurrence of $\rho_Z(T)$ is

$$C(\rho_Z) = \max [|\xi_1 - \xi_3| - \xi_2 - \xi_4, 0], \tag{3.2}$$

where

$$\begin{aligned} \xi_1 &= \frac{1}{Z_Z} e^{\beta[|J_x - J_y| - J_z]} & \xi_2 &= \frac{1}{Z_Z} e^{-\beta[|J_x - J_y| + J_z]} \\ \xi_3 &= \frac{1}{Z_Z} e^{\beta(J_z + \xi)} & \xi_4 &= \frac{1}{Z_Z} e^{\beta(J_z - \xi)}. \end{aligned} \tag{3.3}$$

Before proceeding further, let us consider $X X Z$ model ($J_x = J_y = J$) with DM interaction. In this model, the concurrence becomes

$$C(\rho_Z) = \frac{e^{\beta J_z}}{Z_Z} \max \left[|e^{2\beta w} - e^{-2\beta J_z}| - e^{-2\beta w} - e^{-2\beta J_z}, 0 \right], \tag{3.4}$$

where $w = \sqrt{J^2 + D_z^2}$. This is plotted in Fig. 1a as a function of T and D_z with choosing $J = 1$ and $J_z = 0.2$. As this figure shows, this model exhibits a quantum phase transition with the critical temperature T_c . This means that the entanglement completely vanishes at $T \geq T_c$. From Eq. (3.4), one can show that the critical temperature satisfies

$$e^{2J_z/T_c} \sinh \left(\frac{2w}{T_c} \right) = 1. \tag{3.5}$$

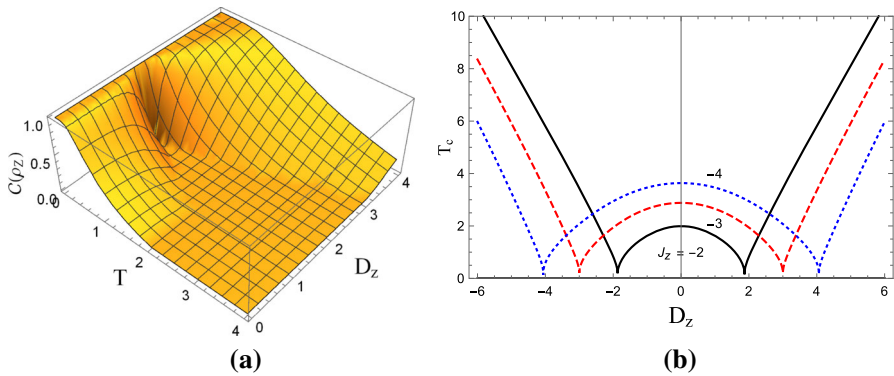


Fig. 2 (Color online) **a** The T - and D_z -dependence of concurrence $C(\rho_Z)$ in $X Y Z$ model with DM interaction when $J_x = -1$, $J_y = -1.5$, and $J_z = -2$. As this figure shows, the concurrence exhibits different behavior in $|D_z| \leq \sqrt{7/2} = 1.87$ and other regions. This is because of the fact that the critical temperature is determined by different equations in these regions [Eq. (3.6)]. **b** The D_z -dependence of the critical temperature T_c when $J_z = -2$ (black line), $J_z = -3$ (red dashed line), and $J_z = -4$ (blue dotted line) with choosing $J_x = -1$ and $J_y = -1.5$. As this figure shows, T_c increases monotonically with increasing $|D_z|$ in the region $|D_z| \geq \sqrt{7/2}$ as $X X Z$ model. However, it behaves differently in the region $|D_z| < \sqrt{7/2}$ as (a) exhibits

Now, let us go back to the $X Y Z$ model with DM interaction. In this model, the critical temperature T_c satisfies

$$\begin{aligned}
 e^{2J_z/T_c} \frac{\sinh(\xi/T_c)}{\cosh(|J_x - J_y|/T_c)} &= 1 \quad \text{when } 2J_z + \xi \geq |J_x - J_y| \\
 e^{-2J_z/T_c} \frac{\sinh(|J_x - J_y|/T_c)}{\cosh(\xi/T_c)} &= 1 \quad \text{when } 2J_z + \xi < |J_x - J_y|. \quad (3.6)
 \end{aligned}$$

When $J_x = J_y$, the first equation reduces to Eq. (3.5) and the second equation does not yield any solution.

For antiferromagnetic ($J_\alpha > 0$) case, the second equation does not play any role because the condition $2J_z + \xi < |J_x - J_y|$ cannot be satisfied. Thus, the behavior of the concurrence $C(\rho_Z)$ is similar to that of $X X Z$ model. The D_z -dependence of T_c is plotted in Fig. 1b when $J_x = 1$ and $J_y = 1.5$ with varying $J_z = 2$ (black line), 3 (red dashed line), and 4 (blue dotted line). Figure 1b shows that T_c increases very rapidly with increasing $|D_z|$. With fixed D_z , T_c increases with increasing J_z .

For ferromagnetic ($J_\alpha < 0$) case, however, the second equation of Eq. (3.6) provides significant solutions, which result in different behavior of $C(\rho_Z)$. The boundary of two region in Eq. (3.6) is $D_z = D_{z,*}$, where

$$D_{z,*} = \sqrt{(J_z - J_>)(J_z + J_<)} \quad (3.7)$$

with $J_> = \max(J_x, J_y)$ and $J_< = \min(J_x, J_y)$. At this point, T_c becomes exactly zero because $\xi_1 = \xi_3$ at this point. In Fig. 2a, we plot $C(\rho_Z)$ as a function of T and D_z with choosing $J_x = -1$, $J_y = -1.5$, and $J_z = -2$. As this figure

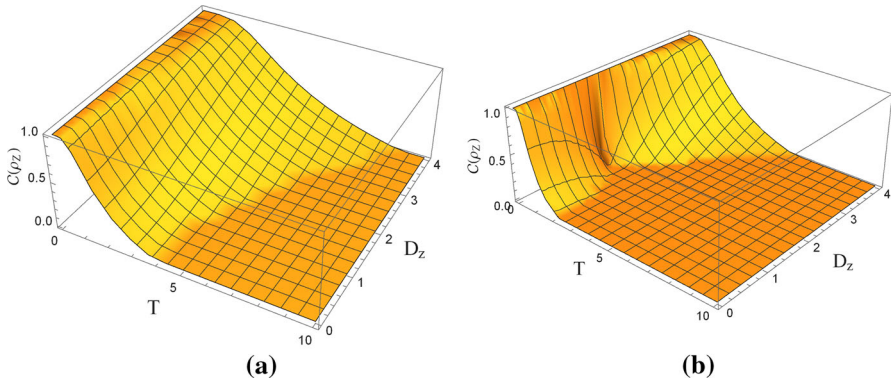


Fig. 3 (Color online) The T - and D_z -dependence of $\mathcal{C}(\rho_Z)$ when $J_x = 3$ and $J_y = 2$ with $J_z = -1$ (a) and $J_z = -2.5$ (b). As expected **a, b** exhibit similar behavior to Figs. 1a and 2a, respectively. This is due to the existence or nonexistence of $D_{z,*}$

shows, the concurrence exhibits different behavior in $0 \leq D_z \leq \sqrt{7/2} = 1.87$ and other regions. This is because of the fact that the second equation of Eq. (3.6) generates the critical temperature in the region $0 \leq D_z \leq \sqrt{7/2}$, while the first equation generates it in other region. In order to show more precisely, we plot the D_z -dependence of T_c in Fig. 2b when $J_z = -2$ (black line), -3 (red dashed line), and -4 (blue dotted line) with fixing $J_x = -1$ and $J_y = -1.5$. As this figure shows, T_c increases monotonically with increasing $|D_z|$ in the region $|D_z| \geq D_{z,*}$ as $X X Z$ model. With fixed D_z , in this region, T_c decreases with increasing $|J_z|$. However, it behaves differently in the region $|D_z| < D_{z,*}$. In this region, T_c decreases with increasing $|D_z|$. With fixed D_z , in this region, T_c increases with increasing $|J_z|$. At $D_z = D_{z,*}$ this figure confirms $T_c = 0$.

For neither ferromagnetic nor antiferromagnetic case, the behavior of the concurrence is determined whether the second equation of Eq. (3.6) plays a role or not. For example, let us consider $J_z > 0$ case. If, in this case, $D_z^2 + J_x J_y \geq 0$, the second equation of Eq. (3.6) does not play any role. Thus, in this case the concurrence is similar to Fig. 1a. If $D_z^2 + J_x J_y < 0$, the condition for the existence of $D_{z,*}$ is $0 < J_z < \min(-J_<, J_>)$. Thus, if both $D_z^2 + J_x J_y < 0$ and $0 < J_z < \min(-J_<, J_>)$ hold, the concurrence of ρ_Z is similar to Fig. 2a. For negative J_z case, one can derive $J_z < \min(-J_<, 0)$ for $J_> > -J_<$ and $J_z < \min(J_>, 0)$ for $-J_< > J_>$ for the existence of $D_{z,*}$. In Fig. 3, we plot D_z - and T -dependence of $\mathcal{C}(\rho_Z)$ when $J_x = 3$ and $J_y = 2$ with $J_z = -1$ (Fig. 3a) and $J_z = -2.5$ (Fig. 3b). As expected, Fig. 3a, b exhibits similar behavior to Figs. 1a and 2a, respectively.

For $\rho_Y(T)$, the concurrence becomes

$$\mathcal{C}(\rho_Y) = \max [|\eta_1 - \eta_3| - \eta_2 - \eta_4, 0], \tag{3.8}$$

where

$$\begin{aligned} \eta_1 &= \frac{1}{Z_Y} e^{\beta[|J_x - J_z| - J_y]} & \eta_2 &= \frac{1}{Z_Y} e^{-\beta[|J_x - J_z| + J_z]} \\ \eta_3 &= \frac{1}{Z_Y} e^{\beta(J_y + \eta)} & \eta_4 &= \frac{1}{Z_Y} e^{\beta(J_y - \eta)}. \end{aligned} \tag{3.9}$$

Unlike $\rho_Z(T)$, even in the $X X Z$ model with DM interaction the critical temperature T_c is determined by two different equations as follows:

$$\begin{aligned} e^{2J/T_c} \frac{\sinh(\eta/T_c)}{\cosh(|J - J_z|/T_c)} &= 1 \quad \text{when } 2J + \eta \geq |J - J_z| \\ e^{-2J/T_c} \frac{\sinh(|J - J_z|/T_c)}{\cosh(\eta/T_c)} &= 1 \quad \text{when } 2J + \eta < |J - J_z|. \end{aligned} \tag{3.10}$$

For the antiferromagnetic case ($J, J_z > 0$), the critical temperature is determined by only the first equation of Eq. (3.10) because $2J + \eta \geq |J - J_z|$ in this case. Thus, the concurrence exhibits similar behavior with that of Fig. 1a. This is confirmed in Fig. 4a, where $\mathcal{C}(\rho_Y)$ is plotted as a function of T and D_y with choosing $J = 3$ and $J_z = 1$. For the ferromagnetic ($J, J_z < 0$) case, however, both equations of Eq. (3.10) play significant role for determining the critical temperature. This is also confirmed in Fig. 4b, where $\mathcal{C}(\rho_Y)$ is plotted as a function of T and D_y with choosing $J = -3$ and $J_z = -1$. In this case, the second equation of Eq. (3.10) determines T_c in the region $|D_y| < 2\sqrt{3} = 3.46$, while T_c in other region is determined by the first equation of Eq. (3.10). In Fig. 4c, the D_y -dependence of T_c is plotted for antiferromagnetic ($J = 3, J_z = 1$) and ferromagnetic ($J = -3, J_z = -1$) cases as black and red dashed lines, respectively. As expected, the critical temperature for ferromagnetic case behaves differently from that for antiferromagnetic case.

For $X Y Z$ model with DM interaction, Eq. (3.10) is replaced with

$$\begin{aligned} e^{2J_y/T_c} \frac{\sinh(\eta/T_c)}{\cosh(|J_x - J_z|/T_c)} &= 1 \quad \text{when } 2J_y + \eta \geq |J_x - J_z| \\ e^{-2J_y/T_c} \frac{\sinh(|J_x - J_z|/T_c)}{\cosh(\eta/T_c)} &= 1 \quad \text{when } 2J_y + \eta < |J_x - J_z|. \end{aligned} \tag{3.11}$$

As in the case of $X X Z$ model, the critical temperature T_c for the antiferromagnetic case is determined by only the first equation of Eq. (3.11). Thus, the behavior of $\mathcal{C}(\rho_Y)$ is similar to Fig. 3a. Of course, both equations are used to determine T_c for ferromagnetic case. The boundary of two regions in Eq. (3.11) is $D_y = D_{y,*}$, where

$$D_{y,*} = \sqrt{(J_y - \tilde{J}_>)(J_y + \tilde{J}_<)} \tag{3.12}$$

with $\tilde{J}_> = \max(J_x, J_z)$ and $\tilde{J}_< = \min(J_x, J_z)$. At this point, T_c becomes zero because $\eta_1 = \eta_3$ as Eq. (3.9) shows.

In Fig. 5, we plot the D_y -dependence of T_c for antiferromagnetic (Fig. 5a) and ferromagnetic (Fig. 5b) cases with varying J_y . In Fig. 5a, we choose $J_x = 1, J_z = 2$, and $J_y = 1.5$ (black line), 2.5 (red dashed line), 3.5 (blue dotted line). Like $\rho_Z(T)$

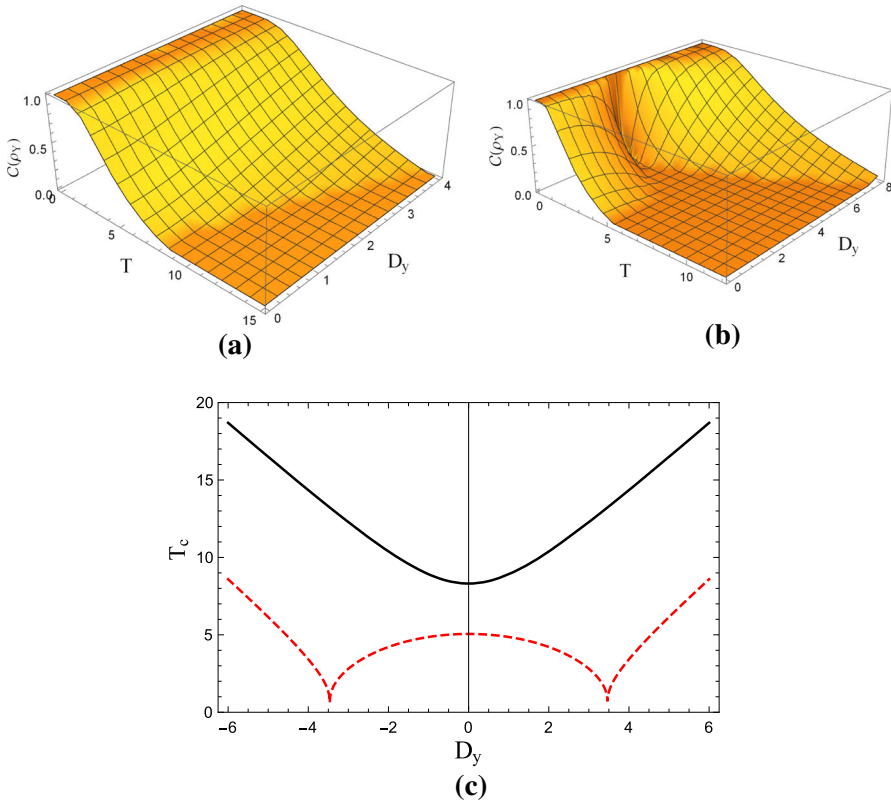


Fig. 4 (Color online) **a** The T - and D_y -dependence of $\mathcal{C}(\rho_Y)$ when $J_x = J_y = 3$ and $J_z = 1$. This behaves very similar to Fig. 1a. This is because of the fact that the critical temperature is determined by single equation. **b** The T - and D_y -dependence of $\mathcal{C}(\rho_Y)$ when $J_x = J_y = -3$ and $J_z = -1$. This behaves very similar to Fig. 2(a). This is because of the fact that the critical temperature is determined by two different equations [Eq. (3.10)]. **c** The D_y -dependence of T_c for antiferromagnetic ($J = 3, J_z = 1$) and ferromagnetic ($J = -3, J_z = -1$) cases as black and red dashed lines, respectively

T_c increases with increasing $|D_y|$. The critical temperature T_c with fixed D_y tends to increase with increasing J_y . In Fig. 5b, we choose $J_x = -1, J_z = -2$, and $J_y = -1.5$ (black line), -2.5 (red dashed line), -3.5 (blue dotted line). At the region $|D_y| \geq D_{y,*}$, T_c increases with increasing $|D_y|$. With fixed D_y , in this region, T_c tends to decrease with increasing $|J_y|$. At the region $|D_y| < D_{y,*}$, T_c decreases with increasing $|D_y|$. With fixed D_y , T_c increases with increasing $|J_y|$.

For nether ferromagnetic and antiferromagnetic case, the behavior of the concurrence is determined whether the second equation of Eq. (3.11) plays a role or not. Since it is similar to that of $D_x = D_y = 0$ case, we will not repeat the analysis.

4 Thermal discord

In this section, we examine the temperature dependence of quantum discord [4,5] for the thermal density matrices $\rho_Z(T)$ and $\rho_Y(T)$.

As quantum entanglement, quantum discord is another measure of quantum correlation for bipartite quantum system. It is defined through discrepancy between two different quantum analogues of classical mutual information. First analogue is

$$I(A : B) = S(A) + S(B) - S(A, B), \tag{4.1}$$

where S denotes a von Neumann entropy $S(\rho) = -\text{Tr}(\rho \log \rho)$. In our paper, all logarithms are taken to base 2. This is a quantum analogue of classical mutual information $I_{cl}(A : B) = H(A) + H(B) - H(A, B)$, where H denotes a Shannon entropy. Another expression of classical mutual information is $I_{cl}(A : B) = H(A) - H(A|B) = H(B) - H(B|A)$, where $H(X|Y)$ is a conditional entropy of X given Y . The quantum analogue of this representation [4] is

$$J(A : B)_{\{\Pi_j^B\}} = S(A) - \sum_j p_j S(A|\Pi_j^B), \tag{4.2}$$

where $\{\Pi_j^B\}$ denotes a complete set of measurement operators prepared by party B and $S(A|\Pi_j^B)$ is a von Neumann entropy of party A after party B obtains a measurement outcome j . As obvious, p_j is the probability of obtaining outcome j in the quantum measurement. The general quantum mechanical postulates [2] imply that

$$p_j = \text{Tr}_{A,B} \left(\Pi_j^B \rho_{AB} \Pi_j^B \right), \quad S \left(A|\Pi_j^B \right) = S \left(\rho \left(A|\Pi_j^B \right) \right), \tag{4.3}$$

where $\rho(A|\Pi_j^B) = \text{Tr}_B(\Pi_j^B \rho_{AB} \Pi_j^B) / p_j$. Hence, unlike $I(A : B)$, $J(A : B)$ is dependent on the complete set of measurement operators. The quantum discord is defined as

$$\begin{aligned} \mathcal{D}(A : B) &= \min [I(A : B) - J(A : B)] \\ &= \min \left[S(B) - S(A, B) + \sum_j p_j S(A|\Pi_j^B) \right], \end{aligned} \tag{4.4}$$

where the minimum is taken over all possible choice of the complete set of measurement operators.⁴

The quantum discord for $\rho_Z(T)$ can be easily computed because it belongs to X -states. The quantum discord for general X -state was computed in Ref. [53,54]. For $\rho_Z(T)$, the last term of Eq. (4.4) becomes

³ Depending on the specific rules about the local operations and classical communication (LOCC) between parties A and B , one can define several different generalizations of $I_{cl}(A : B)$ [51,52]. Thus, several different quantum discords can be defined. Our Definition (4.2) corresponds to the optimal efficiency of a one-way purification strategy [51].

⁴ Although the authors in Ref. [4] consider the projective measurement, the authors in Ref. [5] consider the general measurement including positive operator-valued measure (POVM). Thus, the quantum discord in Ref. [5] is the lower bound of that in [4].

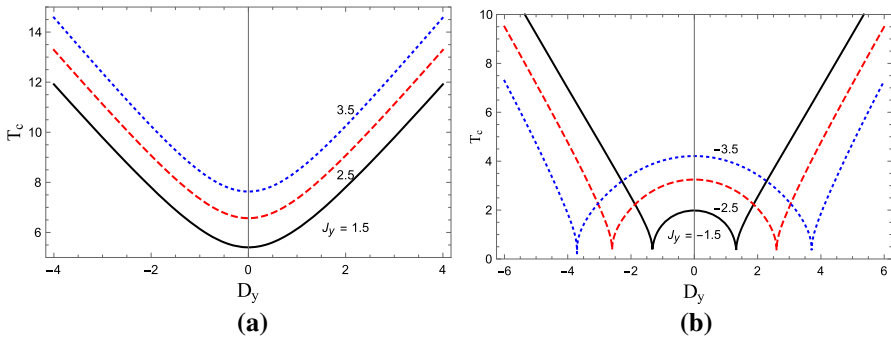


Fig. 5 (Color online) The D_y -dependence of T_c for antiferromagnetic **(a)** and ferromagnetic **(b)** cases with varying J_y . **a** $J_x = 1, J_z = 2$, and $J_y = 1.5$ (black line), 2.5 (red dashed line), 3.5 (blue dotted line) are chosen. **b** $J_x = -1, J_z = -2$, and $J_y = -1.5$ (black line), -2.5 (red dashed line), -3.5 (blue dotted line) are chosen

$$\min_j \sum p_j S(A|\Pi_j^B) = \min(D_{z,1}, D_{z,2}), \tag{4.5}$$

where

$$D_{z,1} = -p \log p - (1 - p) \log(1 - p) \quad D_{z,2} = -2r \log r - 2u \log u - 1 \tag{4.6}$$

with $p = \frac{1}{2} [1 + 2(|s| + |v|)]$. The parameters r, s, u , and v are defined in Eq. (2.7). Thus, quantum discord for $\rho_Z(T)$ is given by

$$\begin{aligned} \mathcal{D}(\rho_Z) &= 1 + (r + s) \log(r + s) + (r - s) \log(r - s) \\ &\quad + (u + |v|) \log(u + |v|) + (u - |v|) \log(u - |v|) \\ &\quad + \min(D_{z,1}, D_{z,2}). \end{aligned} \tag{4.7}$$

In Fig. 6, we plot T - and D_z -dependence of the thermal discord $\mathcal{D}(\rho_Z)$ for (a) antiferromagnetic ($J_x = 1, J_y = 1.5, J_z = 2$) case and (b) ferromagnetic ($J_x = -1, J_y = -1.5, J_z = -2$) case. Although both thermal discords exhibit rapidly damping behavior with increasing T , unlike concurrence they do not reach exact zero. This means that thermal discord does not vanish for separable states. Furthermore, for the ferromagnetic case the thermal discord exhibits an extraordinary behavior at $D_z \approx D_{z,*} = \sqrt{7/2}$ like the concurrence. It seems to form a valley in this region. In order to examine this behavior more precisely, we plot $\mathcal{D}(\rho_Z)$ with choosing $D_z = 0.8$ (red dashed line), 1.8 (black line), 2.8 (blue dotted line) in Fig. 6c without changing J_α . This figure shows that $\mathcal{D}(\rho_Z)$ makes a local minimum at small T region when $D_z = 1.8$, while other cases exhibit exponential damping behavior without local minimum. At $D_z = D_{z,*}$ and $T = 0$, one can show $r = u = |v| = 1/4$ and $s = \mp 1/4$, which result in $D_{z,1} = 0$ and $D_{z,2} = 1$. Thus, the thermal discord of $\rho_Z(T)$ is exactly zero when $D_z = D_{z,*}$ and $T = 0$. Since $T_c = 0$ at $D_z = D_{z,*}$, both thermal entanglement and thermal discord simultaneously vanish at this point.

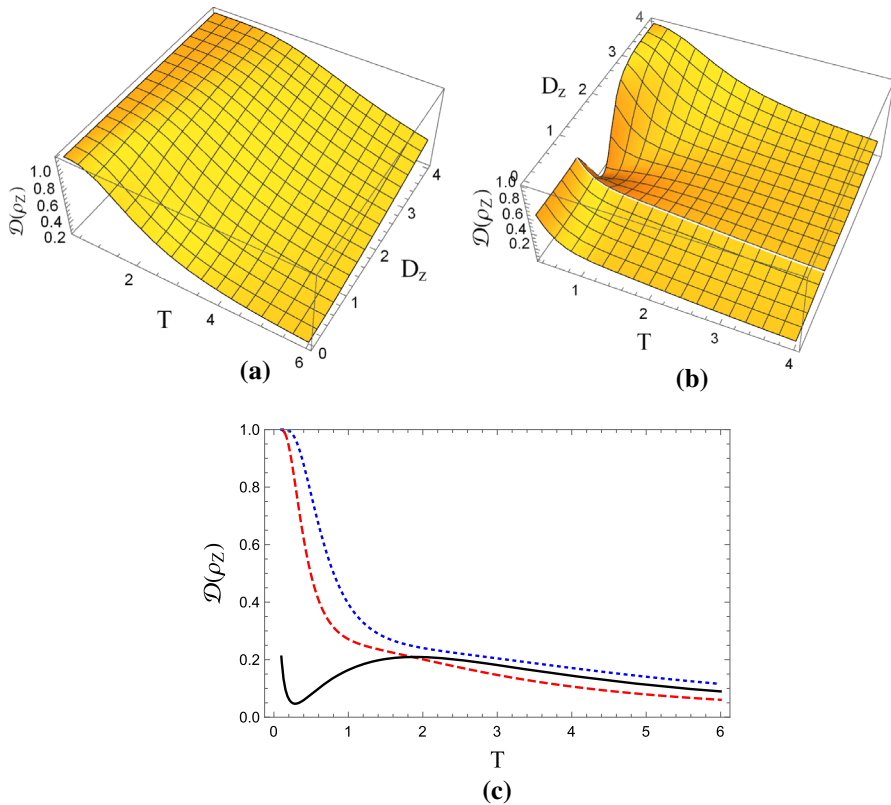


Fig. 6 (Color online) The T - and D_z -dependence of the thermal discord $\mathcal{D}(\rho_Z)$ for **a** antiferromagnetic ($J_x = 1, J_y = 1.5, J_z = 2$) case and **b** ferromagnetic ($J_x = -1, J_y = -1.5, J_z = -2$) case. In order to examine the behavior of $\mathcal{D}(\rho_Z)$ for ferromagnetic case at $D_z \approx \sqrt{7}/2$, $\mathcal{D}(\rho_Z)$ is plotted in **(c)** with choosing $D_z = 0.8$ (red dashed line), 1.8 (black line), 2.8 (blue dotted line) without changing J_α

Since $\rho_Y(T)$ does not belong to X -states, its thermal discord should be computed explicitly. This is carried out in “Appendix A,” which gives

$$\mathcal{D}(\rho_Y) = 1 + \sum_{i=1}^4 \frac{e^{-E_{i,y}/T}}{\mathcal{Z}_Y} \log \left(\frac{e^{-E_{i,y}/T}}{\mathcal{Z}_Y} \right) + h \left(\frac{1}{2} + \sqrt{y_{\max}} \right), \quad (4.8)$$

where $h(p) = -p \log p - (1 - p) \log(1 - p)$ and

$$y_{\max} = \frac{1}{2} \left[8q^2 + (r_1 - u_1)^2 + (r_2 + u_2)^2 + |(r_1 - u_1) - (r_2 + u_2)| \sqrt{16q^2 + [(r_1 - u_1) + (r_2 + u_2)]^2} \right]. \quad (4.9)$$

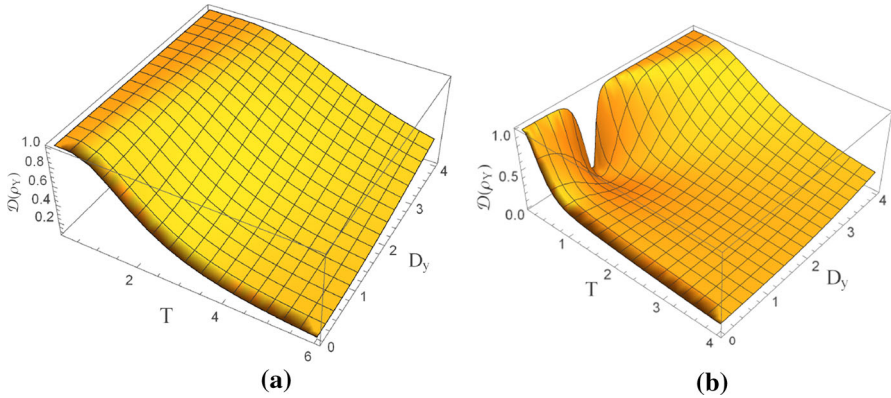


Fig. 7 (Color online) The T - and D_y -dependence of the thermal discord $\mathcal{D}(\rho_Y)$ for **a** antiferromagnetic ($J_x = 1, J_y = 1.5, J_z = 2$) case and **b** ferromagnetic ($J_x = -1, J_y = -1.5, J_z = -2$) case. For the ferromagnetic case, the thermal discord exhibits an extraordinary behavior at $D_y \approx D_{y,*} = \sqrt{7}/2 = 1.32$ like Fig. 6b

In Fig. 7, we plot T - and D_y -dependence of the thermal discord $\mathcal{D}(\rho_Y)$ for (a) antiferromagnetic ($J_x = 1, J_y = 1.5, J_z = 2$) case and (b) ferromagnetic ($J_x = -1, J_y = -1.5, J_z = -2$) case. Like Fig. 6, both thermal discords do not reach exact zero in spite of exponential damping with increasing T . For the ferromagnetic case, the thermal discord exhibits an extraordinary behavior at $D_y \approx D_{y,*} = \sqrt{7}/2 = 1.32$ like Fig. 6b.

Finally, we plot in Fig. 8 that (a) the D_z -dependence of $\mathcal{D}(\rho_Z)$ and (b) D_y -dependence of $\mathcal{D}(\rho_Y)$ at $T = T_c$. In both figures, red solid and blue dashed lines correspond to ferromagnetic ($J_x = -1, J_y = -1.5, J_z = -2$) and antiferromagnetic ($J_x = 1, J_y = 1.5, J_z = 2$) cases, respectively. Thus, these figures show the discrepancy between thermal discord and thermal entanglement because concurrence at $T = T_c$ is exactly zero. Within the range $0 \leq D_z, D_y \leq 4$, these figures show $\mathcal{D}(\rho_Z) \approx \mathcal{D}(\rho_Y) \approx 0.1$ for both antiferromagnetic cases. For ferromagnetic cases, $\mathcal{D}(\rho_Z)$ and $\mathcal{D}(\rho_Y)$ fall to zero at $D_z = \sqrt{7}/2$ and $\sqrt{7}/2$ at $T = T_c$. This fact implies that for arbitrary ferromagnetic cases ($J_\alpha < 0$) both thermal discord and thermal entanglement simultaneously vanish at $D_z = D_{z,*}$ for $\rho_Z(T_c)$ and $D_y = D_{y,*}$ for $\rho_Y(T_c)$. If one extends the range of D_z and D_y in Fig. 8, both antiferromagnetic and ferromagnetic $\mathcal{D}(\rho_Z)$ and $\mathcal{D}(\rho_Y)$ approach to one for $D_z, D_y \rightarrow \pm\infty$. Thus, maximal discrepancy between thermal discord and thermal entanglement occurs in this limit at the critical temperature.

5 Conclusions

We derive explicitly the thermal density matrices $\rho_Z(T)$ and $\rho_Y(T)$ for two-qubit Heisenberg $X Y Z$ chain with DM interaction in the z - or y -direction. For each density matrix, the thermal entanglement expressed by $\mathcal{C}(\rho_Z)$ or $\mathcal{C}(\rho_Y)$ is explicitly computed. Exploiting the explicit expressions of $\mathcal{C}(\rho_Z)$ or $\mathcal{C}(\rho_Y)$, we discuss on the quantum phase

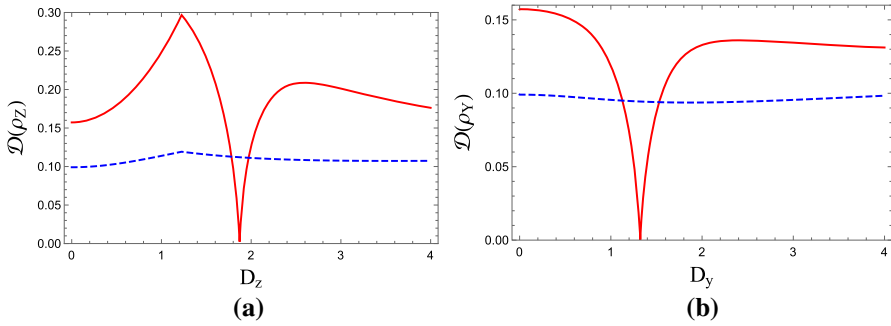


Fig. 8 (Color online) **a** The D_z -dependence of $\mathcal{D}(\rho_Z)$ and **b** D_y -dependence of $\mathcal{D}(\rho_Y)$ at $T = T_c$. In both figures, red solid and blue dashed lines correspond to ferromagnetic ($J_x = -1, J_y = -1.5, J_z = -2$) and antiferromagnetic ($J_x = 1, J_y = 1.5, J_z = 2$) cases, respectively

transition in detail. In particular, we focus on the critical temperature T_c , above which the thermal entanglement completely vanishes. This means that each density matrix becomes separable state at $T \geq T_c$.⁵

For antiferromagnetic case ($J_\alpha > 0, \alpha = x, y, z$), the critical temperature is determined by single equation for each thermal density matrix. As a result, T_c monotonically increases with increasing $|D_z|$ or $|D_y|$. For ferromagnetic case, ($J_\alpha < 0, \alpha = x, y, z$), however, the situation is different. In this case, the critical temperature is determined by two different equations in the two separate regions. For $\rho_Z(T)$, for example, these two separate regions are defined by $|D_z| < D_{z,*}$ and $|D_z| \geq D_{z,*}$. Similarly, the two separate regions for $\rho_Y(T)$ are given by $|D_y| < D_{y,*}$ and $|D_y| \geq D_{y,*}$. At the outer region $|D_z| \geq D_{z,*}$ or $|D_y| \geq D_{y,*}$ the critical temperature T_c monotonically increases with increasing $|D_z|$ or $|D_y|$ like antiferromagnetic case. At the inner region $|D_z| < D_{z,*}$ or $|D_y| < D_{y,*}$, however, T_c decreases with increasing $|D_z|$ or $|D_y|$. As a result, the D_α - ($\alpha = z, y$) and T -dependence of thermal entanglements for ferromagnetic case exhibit different behavior from those for antiferromagnetic case.

Thermal discords $\mathcal{D}(\rho_Z)$ and $\mathcal{D}(\rho_Y)$ for $\rho_Z(T)$ and $\rho_Y(T)$ are explicitly derived. For antiferromagnetic case with fixed D_z or D_y , both $\mathcal{D}(\rho_Z)$ and $\mathcal{D}(\rho_Y)$ exhibit exponential damping behavior with increasing T , but they do not reach exact zero. For ferromagnetic case, both $\mathcal{D}(\rho_Z)$ and $\mathcal{D}(\rho_Y)$ exhibit extraordinary behavior at $|D_z| \approx D_{z,*}$ and $|D_y| \approx D_{y,*}$. In these regions, the T -dependence of $\mathcal{D}(\rho_Z)$ or $\mathcal{D}(\rho_Y)$ involves local minimum at small T , while in other region they exhibit exponential damping behavior without local minimum. Although definitions of quantum entanglement and quantum discord are completely different, one can infer from our results that they exhibit similar behavior with each other because for ferromagnetic case both exhibit extraordinary behavior at the regions $|D_z| \approx D_{z,*}$ and $|D_y| \approx D_{y,*}$. At $D_z = D_{z,*}$ or $D_y = D_{y,*}$ both thermal entanglement and thermal discord for $\rho_Z(T)$ or $\rho_Y(T)$ simultaneously vanish at $T = T_c = 0$.

⁵ Of course, this critical behavior of entanglement occurs when the DM interaction has arbitrary direction. In order to show this fact more explicitly, we discuss the critical behavior in ‘‘Appendix B’’ when $D_x \neq 0$ and $D_y \neq 0$.

One can apply our analysis when external magnetic field \mathbf{B} is applied to our system [38]. In this case, the Hamiltonian is changed into

$$H_T = H + \mathbf{B} \cdot (\boldsymbol{\sigma}_1 + \boldsymbol{\sigma}_2), \quad (5.1)$$

where H is given in Eq. (2.1). It seems to be of interest to examine the effect of external magnetic field and DM coupling constants in the thermal entanglement and thermal discord. In particular, it is of interest to analyze the behavior of thermal discord near the critical temperature in this model.

Another interesting issue is to examine the quantum phase transition by introducing 3-spin Heisenberg model with DM interaction, whose Hamiltonian is

$$H_3 = \sum_{i=1}^2 [J_x \sigma_i^x \otimes \sigma_{i+1}^x + J_y \sigma_i^y \otimes \sigma_{i+1}^y + J_z \sigma_i^z \otimes \sigma_{i+1}^z + \mathbf{D} \cdot (\boldsymbol{\sigma}_i \times \boldsymbol{\sigma}_{i+1})]. \quad (5.2)$$

The tripartite entanglement was introduced in Ref. [55,56]. It is of interest to compute the thermal tripartite entanglement and to discuss on the quantum phase transition. It seems to be of interest to examine how the monogamy relation is changed with varying DM coupling constants and external temperature.

One can extend our analysis to continuum system. For example, let us consider two coupled harmonic oscillator system, whose Hamiltonian is

$$H = \frac{1}{2} (\dot{x}_1^2 + \dot{x}_2^2) + \frac{1}{2} (\omega_1^2 x_1^2 + \omega_2^2 x_2^2) - J x_1 x_2. \quad (5.3)$$

In this case, the thermal density matrix $\rho(x'_1, x'_2 : x_1, x_2 : T)$ can be derived exactly by making use of diagonalization of Hamiltonian and Euclidean path integral technique [57]. This thermal density matrix is generally mixed state. For mixed state, entanglement is in general defined via a convex roof method [58,59]:

$$\mathcal{E}(\rho) = \min \sum_j p_j \mathcal{E}(\psi_j), \quad (5.4)$$

where minimum is taken over all possible pure state decompositions, i.e., $\rho = \sum_j p_j |\psi_j\rangle\langle\psi_j|$, with $0 \leq p_j \leq 1$. However, we do not know how to derive the optimal decomposition for continuum thermal density matrix $\rho(x'_1, x'_2 : x_1, x_2 : T)$. We would like to explore this issue in the future.

Acknowledgements This work was supported by the Kyungnam University Foundation Grant, 2017.

Appendix A

In this appendix, we compute the thermal discord for $\rho_Y(T)$ given in Eq. (2.11). We define the measurement operators Π_j^B as $\Pi_j^B = |B_j\rangle\langle B_j| (j = 1, 2)$, where

$$|B_1\rangle = \cos \frac{\theta}{2} |0\rangle + e^{i\phi} \sin \frac{\theta}{2} |1\rangle \quad |B_2\rangle = \sin \frac{\theta}{2} |0\rangle - e^{i\phi} \cos \frac{\theta}{2} |1\rangle. \tag{A.1}$$

For our purpose, θ and ϕ are confined as $0 \leq \theta \leq \pi/2, 0 \leq \phi < 2\pi$.

Then, it is straightforward to show $G(\theta, \phi) = \sum_j p_j S(A|\Pi_j^B)$ becomes

$$G(\theta, \phi) = - \left(\frac{1}{2} + \sqrt{y} \right) \log \left(\frac{1}{2} + \sqrt{y} \right) - \left(\frac{1}{2} - \sqrt{y} \right) \log \left(\frac{1}{2} - \sqrt{y} \right), \tag{A.2}$$

where

$$y = \left[(r_1 - u_1)^2 + 4q^2 \right] \cos^2 \theta + \left[4q^2 \cos^2 \phi + r_2^2 + u_2^2 + 2r_2 u_2 \cos 2\phi \right] \sin^2 \theta + 4q [(r_2 + u_2) - (r_1 - u_1)] \sin \theta \cos \theta \cos \phi. \tag{A.3}$$

The parameters r_1, r_2, u_1, u_2 , and q are explicitly given in Eq. (2.12).

Now, we should minimize $G(\theta, \phi)$. We should note that $G(\theta, \phi)$ is a type of binary entropy function $h(p) = -p \log p - (1-p) \log(1-p)$, which is concave with respect to p and attains its maximum value of one at $p = 1/2$. Thus, minimizing $G(\theta, \phi)$ is exactly the same with maximizing y , i.e.,

$$\frac{\partial y(\theta, \phi)}{\partial \theta} = 0 \quad \frac{\partial y(\theta, \phi)}{\partial \phi} = 0. \tag{A.4}$$

$\partial y(\theta, \phi)/\partial \phi = 0$ yields three solutions

$$\sin \theta = 0 \quad \sin \phi = 0 \quad \tan \theta = \frac{q[(r_1 - u_1) - (r_2 + u_2)]}{2 \cos \phi (q^2 + r_2 u_2)}, \tag{A.5}$$

and $\partial y(\theta, \phi)/\partial \theta = 0$ yields

$$\tan 2\theta = - \frac{4q \cos \phi [(r_1 - u_1) - (r_2 + u_2)]}{4(q^2 + r_2 u_2) \sin^2 \phi + (r_1 - u_1)^2 - (r_2 + u_2)^2}. \tag{A.6}$$

The solution $\sin \theta = 0$ and Eq. (A.6) make y to be

$$y_1 = (r_1 - u_1)^2 + 4q^2. \tag{A.7}$$

The solution $\sin \phi = 0$ and Eq. (A.6) generate two y and larger one is

$$y_2 = \frac{1}{2} \left[8q^2 + (r_1 - u_1)^2 + (r_2 + u_2)^2 + |(r_1 - u_1) - (r_2 + u_2)| \sqrt{16q^2 + [(r_1 - u_1) + (r_2 + u_2)]^2} \right]. \tag{A.8}$$

In order for the third solution of Eqs. (A.5) and (A.6) to be consistent, we need a condition

$$4(q^2 + r_2u_2)^2 + [(r_1 - u_1) - (r_2 + u_2)][2q^2(r_2 + u_2) + r_2u_2\{(r_1 - u_1) + (r_2 + u_2)\}] = 0$$

identically because $\tan 2\theta = 2 \tan \theta / (1 - \tan^2 \theta)$. However, one can show easily that this condition does not hold identically by making use of Eq. (2.12). There is another possibility. The boundary value of y can be maximum although it is not local maximum. Thus, another candidate for $\max y$ is y at $\theta = \pi/2, \phi = 0$, which is

$$y_3 = (r_2 + u_2)^2 + 4q^2. \tag{A.9}$$

It is easy to show $y_{\max} = \max(y_1, y_2, y_3) = y_2$. Thus, $\min G(\theta, \phi)$ becomes

$$\begin{aligned} \min G(\theta, \phi) = & - \left(\frac{1}{2} + \sqrt{y_2} \right) \log \left(\frac{1}{2} + \sqrt{y_2} \right) \\ & - \left(\frac{1}{2} - \sqrt{y_2} \right) \log \left(\frac{1}{2} - \sqrt{y_2} \right). \end{aligned} \tag{A.10}$$

Appendix B

In this appendix, we will show that the ESD phenomenon of entanglement still occurs when multiple DM components are present. For simplicity, we choose $J_x = J_y \equiv J$ and $D_z = 0$. In this case the Hamiltonian becomes

$$H_{XY} = \begin{pmatrix} J_z & iD_x + D_y & -iD_x - D_y & 0 \\ -iD_x + D_y & -J_z & 2J & iD_x + D_y \\ iD_x - D_y & 2J & -J_z & -iD_x - D_y \\ 0 & -iD_x + D_y & iD_x - D_y & J_z \end{pmatrix}. \tag{B.1}$$

The eigenvalues and corresponding eigenvectors of H_{XY} are summarized in Table 3. In this table, ζ, \mathcal{N}_3 , and \mathcal{N}_4 are given by

$$\begin{aligned} \zeta &= \sqrt{4(D_x^2 + D_y^2) + (J + J_z)^2} \\ \mathcal{N}_3^2 &= 4\zeta \{ \zeta - (J + J_z) \} \quad \mathcal{N}_4^2 = 4\zeta \{ \zeta + (J + J_z) \}. \end{aligned} \tag{B.2}$$

Table 3 Eigenvalues and eigenvectors of H_{XY}

Eigenvalues of H_{XY}	Corresponding eigenvectors
$E_1 = 2J - J_z$	$ E_1\rangle = \frac{1}{\sqrt{2}} (01\rangle + 10\rangle)$
$E_2 = J_z$	$ E_2\rangle = \frac{1}{\sqrt{2}} \left(\sqrt{\frac{D_x - iD_y}{D_x + D_y}} 00\rangle + \sqrt{\frac{D_x + iD_y}{D_x - iD_y}} 11\rangle \right)$
$E_3 = -J + \zeta$	$ E_3\rangle = \frac{1}{\mathcal{N}_3} \left[2(-D_x + iD_y) 00\rangle - i(J + J_z - \zeta)(01\rangle - 10\rangle) + 2(D_x + iD_y) 11\rangle \right]$
$E_4 = -J - \zeta$	$ E_4\rangle = \frac{1}{\mathcal{N}_4} \left[2(-D_x + iD_y) 00\rangle - i(J + J_z + \zeta)(01\rangle - 10\rangle) + 2(D_x + iD_y) 11\rangle \right]$

Thus, the spectral decomposition of H_{XY} can be written as

$$H_{XY} = \sum_{i=1}^4 E_i |E_i\rangle \langle E_i|. \tag{B.3}$$

Then, the partition of this system is

$$\mathcal{Z}_{XY} = \text{Tr}[e^{-\beta H_{XY}}] = 2e^{-\beta J} \cosh[\beta(J - J_z)] + 2e^{\beta J} \cosh(\beta\zeta). \tag{B.4}$$

Then, the thermal density matrix in this case becomes

$$\rho_{XY}(T) = \begin{pmatrix} z_1 & z_3 & -z_3 & z_4 \\ z_3^* & z_2 & z_5 & z_3 \\ -z_3^* & z_5 & z_2 & -z_3 \\ z_4^* & z_3^* & -z_3^* & z_1 \end{pmatrix}, \tag{B.5}$$

where

$$\begin{aligned} z_1 &= \frac{1}{2\mathcal{Z}_{XY}} \left[e^{-\beta J_z} + \frac{e^{\beta J}}{\zeta} \{ \zeta \cosh(\beta\zeta) - (J + J_z) \sinh(\beta\zeta) \} \right] \\ z_2 &= \frac{1}{2\mathcal{Z}_{XY}} \left[e^{-\beta(2J - J_z)} + \frac{e^{\beta J}}{\zeta} \{ \zeta \cosh(\beta\zeta) + (J + J_z) \sinh(\beta\zeta) \} \right] \\ z_3 &= \frac{1}{\mathcal{Z}_{XY}} \frac{-i(D_x - iD_y)}{\zeta} e^{\beta J} \sinh(\beta\zeta) \\ z_4 &= \frac{1}{2\mathcal{Z}_{XY}} \frac{D_x - iD_y}{D_x + iD_y} \left[e^{-\beta J_z} - \frac{e^{\beta J}}{\zeta} \{ \zeta \cosh(\beta\zeta) - (J + J_z) \sinh(\beta\zeta) \} \right] \\ z_5 &= \frac{1}{2\mathcal{Z}_{XY}} \left[e^{-\beta(2J - J_z)} - \frac{e^{\beta J}}{\zeta} \{ \zeta \cosh(\beta\zeta) + (J + J_z) \sinh(\beta\zeta) \} \right]. \end{aligned} \tag{B.6}$$

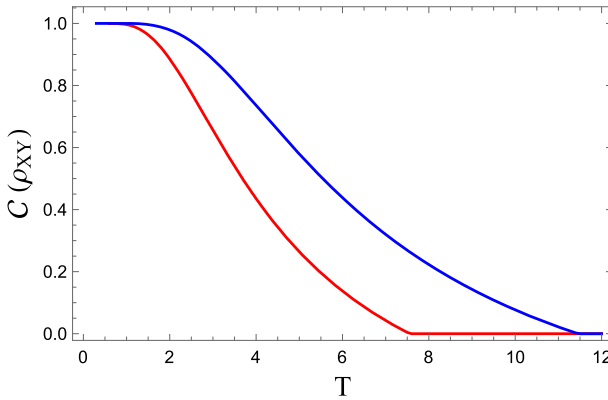


Fig. 9 (Color online) The T -dependence of concurrence with $D = \sqrt{5}$ (red line) and $D = \sqrt{17}$ (blue line) when $J = 1$ and $J_z = 2$. As expected, both decrease with increasing T , and eventually go to zero. The critical temperature is $T_c \sim 7.6$ for $D = \sqrt{5}$ and $T_c \sim 11.5$ for $D = \sqrt{17}$ approximately

In order to compute the concurrence, we should compute the eigenvalues of $R = \rho_{XY}(\sigma_y \otimes \sigma_y)\rho_{XY}^*(\sigma_y \otimes \sigma_y)$. One eigenvalue is $(z_2 + z_5)^2$, and the remaining three eigenvalues are roots of the following cubic equation:

$$\Lambda^3 - \alpha_1\Lambda^2 + \alpha_2\Lambda - \alpha_3 = 0, \tag{B.7}$$

where

$$\begin{aligned} \alpha_1 &= 2z_1^2 + 8a_1 + 2a_2 + a_4^2 \\ \alpha_2 &= z_1^4 + (4a_1 + a_2)^2 - 8z_1a_3 - 4a_3a_4 \\ &\quad + 8z_1a_1(z_1 - a_4) - 2a_2(z_1^2 - a_4^2) + 2z_1^2a_4^2 \\ \alpha_3 &= [2a_3 - 4z_1a_1 + (z_1^2 - a_2)a_4]^2 \end{aligned} \tag{B.8}$$

with

$$a_1 = |z_3|^2 a_2 = |z_4|^2 a_3 = z_3^2 z_4^* + (z_3^*)^2 z_4 a_4 = z_2 - z_5. \tag{B.9}$$

It is worthwhile noting that the D_x - and D_y -dependence of the eigenvalues are only via $D = \sqrt{D_x^2 + D_y^2}$. Thus, the concurrence $\mathcal{C}(\rho_{XY})$ has rotation symmetry in (D_x, D_y) -plane.

Solving the cubic equation (B.7) on the analytical ground is very cumbersome work, because the roots have too long expressions. Thus, we rely on the numerical method from the present stage. The T -dependence of $\mathcal{C}(\rho_{XY})$ with $(D_x = 1, D_y = 2)$ and $(D_x = 1, D_y = 4)$ is plotted in Fig. 9 as red and blue lines, respectively, when $J = 1$ and $J_z = 2$. As expected, both decrease with increasing T and eventually go to zero. The critical temperature is $T_c \sim 7.6$ for $(D_x = 1, D_y = 2)$ and $T_c \sim 11.5$ for $(D_x = 1, D_y = 4)$ approximately.

References

1. Schrödinger, E.: Die gegenwärtige situation in der quantenmechanik. *Naturwissenschaften* **23**, 807 (1935)
2. Nielsen, M.A., Chuang, I.L.: *Quantum Computation and Quantum Information*. Cambridge University Press, Cambridge (2000)
3. Horodecki, R., Horodecki, P., Horodecki, M., Horodecki, K.: Quantum entanglement. *Rev. Mod. Phys.* **81**, 865 (2009). [arXiv:quant-ph/0702225](https://arxiv.org/abs/quant-ph/0702225)
4. Ollivier, H., Zurek, W.H.: Quantum discord: a measure of the quantumness of correlations. *Phys. Rev. Lett.* **88**, 017901 (2002). [arXiv:quant-ph/0105072](https://arxiv.org/abs/quant-ph/0105072)
5. Henderson, L., Vedral, V.: Classical, quantum, and total correlations. *J. Phys. A: Math. Theor.* **34**, 6899 (2001). [[quant-ph/0105028](https://arxiv.org/abs/quant-ph/0105028)]
6. Bennett, C.H., Brassard, G., Crepeau, C., Jozsa, R., Peres, A., Wootters, W.K.: Teleporting an unknown quantum state via dual classical and Einstein–Podolsky–Rosen channels. *Phys. Rev. Lett.* **70**, 1895 (1993)
7. Bennett, C.H., Wiesner, S.J.: Communication via one- and two-particle operators on Einstein–Podolsky–Rosen states. *Phys. Rev. Lett.* **69**, 2881 (1992)
8. Scarani, V., Lblisdir, S., Gisin, N., Acin, A.: Quantum cloning. *Rev. Mod. Phys.* **77**, 1225 (2005). [arXiv:quant-ph/0511088](https://arxiv.org/abs/quant-ph/0511088)
9. Ekert, A.K.: Quantum cryptography based on Bells theorem. *Phys. Rev. Lett.* **67**, 661 (1991)
10. Kollmitzer, C., Pivk, M.: *Applied Quantum Cryptography*. Springer, Heidelberg (2010)
11. Wang, K., Wang, X., Zhan, X., Bian, Z., Li, J., Sanders, B.C., Xue, P.: Entanglement-enhanced quantum metrology in a noisy environment. *Phys. Rev.* **A97**, 042112 (2018). [arXiv:1707.08790](https://arxiv.org/abs/1707.08790)
12. Vidal, G.: Efficient classical simulation of slightly entangled quantum computations. *Phys. Rev. Lett.* **91**, 147902 (2003). [arXiv:quant-ph/0301063](https://arxiv.org/abs/quant-ph/0301063)
13. Ladd, T.D., Jelezko, F., Laflamme, R., Nakamura, Y., Monroe, C., O’Brien, J.L.: Quantum computers. *Nature* **464**, 45 (2010). [arXiv:1009.2267](https://arxiv.org/abs/1009.2267)
14. Ghernaoui-Helie, S., Tashi, I., Laenger, T., Monyk, C.: SECOQC Business White Paper. [arXiv:0904.4073](https://arxiv.org/abs/0904.4073)
15. Zurek, W.H.: Decoherence, einselection, and the quantum origins of the classical. *Rev. Mod. Phys.* **75**, 715 (2003). [arXiv:quant-ph/0105127](https://arxiv.org/abs/quant-ph/0105127)
16. Yu, T., Eberly, J.H.: Finite-time disentanglement via spontaneous emission. *Phys. Rev. Lett.* **93**, 140404 (2004). [arXiv:quant-ph/0404161](https://arxiv.org/abs/quant-ph/0404161)
17. Yu, T., Eberly, J.H.: Sudden death of entanglement: classical noise effects. *Opt. Commun.* **264**, 393 (2006). [arXiv:quant-ph/0602196](https://arxiv.org/abs/quant-ph/0602196)
18. Yu, T., Eberly, J.H.: Quantum open system theory: bipartite aspects. *Phys. Rev. Lett.* **97**, 140403 (2006). [arXiv:quant-ph/0603256](https://arxiv.org/abs/quant-ph/0603256)
19. Yu, T., Eberly, J.H.: Sudden death of entanglement. *Science* **323**, 598 (2009). [arXiv:0910.1396](https://arxiv.org/abs/0910.1396)
20. Almeida, M.P., et al.: Environment-induced sudden death of entanglement. *Science* **316**, 579 (2007). [arXiv:quant-ph/0701184](https://arxiv.org/abs/quant-ph/0701184)
21. Dzyaloshinsky, I.: A thermodynamic theory of “weak” ferromagnetism of antiferromagnetics. *J. Phys. Chem. Solids* **4**, 241 (1958)
22. Moriya, T.: Anisotropic superexchange interaction and weak ferromagnetism. *Phys. Rev.* **120**, 91 (1960)
23. Milivojević, M., Stepanenko, D.: Effective spin Hamiltonian of a gated triple quantum dot in the presence of spin–orbit interaction. *J. Phys.: Condens. Matter* **29**, 405302 (2017)
24. Kane, B.E.: A silicon-based nuclear spin quantum computer. *Nature (London)* **393**, 133 (1998)
25. Loss, D., DiVincenzo, D.P.: Quantum computation with quantum dots. *Phys. Rev. A* **57**, 120 (1998)
26. Burkard, G., Loss, D., DiVincenzo, D.P.: Coupled quantum dots as quantum gates. *Phys. Rev. B* **59**, 2070 (1999)
27. Trauzettel, B., Denis, V., Loss, Bulaev, D., Burkard, Guido: Spin qubits in graphene quantum dots. *Nat. Phys.* **3**, 192 (2007)
28. Senthil, T., Marston, J.B., Fisher, Matthew P.A.: Spin quantum Hall effect in unconventional superconductors. *Phys. Rev. B* **60**, 4245 (1999)
29. Nishiyama, M., Inada, Y., Zheng, G.: Spin triplet superconducting state due to broken inversion symmetry in $\text{Li}_2\text{Pt}_3\text{B}$. *Phys. Rev. Lett.* **98**, 047002 (2007)

30. Sorensen, A., Molmer, K.: Spin–spin interaction and spin squeezing in an optical lattice. *Phys. Rev. Lett.* **83**, 2274 (1999)
31. Radhakrishnan, C., Parthasarathy, M., Jambulingam, S., Byrnes, T.: Quantum coherence of the Heisenberg spin models with Dzyaloshinsky–Moriya interactions. *Sci. Rep.* **7**, 1 (2017). [arXiv:1709.03215](https://arxiv.org/abs/1709.03215)
32. Shekhtman, L., Entin-Wohlman, O., Aharony, Amnon: Moriyas anisotropic superexchange interaction, frustration, and Dzyaloshinskys weak ferromagnetism. *Phys. Rev. Lett.* **69**, 836 (1992)
33. Gangadharaiah, S., Sun, J., Starykh, O.A.: Spin–orbit-mediated anisotropic spin interaction in interacting electron systems. *Phys. Rev. Lett.* **100**, 156402 (2008)
34. Milivojević, M.: Symmetric spin–orbit interaction in triple quantum dot and minimization of spinorbit leakage in CNOT gate. *J. Phys.: Condens. Matter* **30**, 085302 (2018)
35. Zhang, G.F.: Thermal entanglement and teleportation in a two-qubit Heisenberg chain with Dzyaloshinski–Moriya anisotropic antisymmetric interaction. *Phys. Rev. A* **75**, 034304 (2007). [arXiv:quant-ph/0703019](https://arxiv.org/abs/quant-ph/0703019)
36. Li, D.C., Wang, X.P., Cao, Z.L.: Thermal entanglement in the anisotropic Heisenberg XXZ model with the Dzyaloshinskii–Moriya interaction. *J. Phys.: Condens. Matter.* **20**, 325229 (2008). [arXiv:0804.4820](https://arxiv.org/abs/0804.4820)
37. Kargarian, M., Jafari, R., Langari, A.: Dzyaloshinskii–Moriya interaction and anisotropy effects on the entanglement of the Heisenberg model. *Phys. Rev. A* **79**, 042319 (2009). [arXiv:0903.0630](https://arxiv.org/abs/0903.0630)
38. Li, D.C., Cao, Z.L.: Entanglement in the anisotropic Heisenberg XYZ model with different Dzyaloshinskii–Moriya interaction and inhomogeneous magnetic field. *Eur. Phys. J.* **D50**, 207 (2008). [arXiv:0907.1433](https://arxiv.org/abs/0907.1433)
39. Jafari, R., Langari, A.: Three-qubit ground state and thermal entanglement of Heisenberg (XXZ) and Ising models with Dzyaloshinskii–Moriya interaction. *Int. J. Quant. Inf.* **9**, 1057 (2011). [arXiv:0903.2556](https://arxiv.org/abs/0903.2556)
40. Milivojević, M.: Maximal thermal entanglement using three-spin interactions. *Quant. Inf. Proc.* **18**, 48 (2019)
41. Yi-Xin, C., Zhi, Y.: Thermal quantum discord in anisotropic Heisenberg XXZ model with Dzyaloshinskii–Moriya interaction. *Commun. Theor. Phys.* **54**, 60 (2010). [arXiv:1002.0176](https://arxiv.org/abs/1002.0176)
42. Zidan, N.: Quantum discord of a two-qubit anisotropy XXZ Heisenberg chain with Dzyaloshinskii–Moriya interaction. *J. Quant. Inf. Sci.* **4**, 104 (2014)
43. Liu, B.Q., Shao, B., Li, J.G., Zou, J., Wu, L.A.: Quantum and classical correlations in the one-dimensional XY model with Dzyaloshinskii–Moriya interaction. *Phys. Rev.* **A83**, 052112 (2011). [arXiv:1012.2788](https://arxiv.org/abs/1012.2788)
44. Renes, J.M., Boileau, J.C.: Conjectured strong complementary information tradeoff. *Phys. Rev. Lett.* **103**, 020402 (2009). [arXiv:0806.3984](https://arxiv.org/abs/0806.3984)
45. Berta, M., Christandl, M., Colbeck, R., Renes, J.M., Renner, R.: The uncertainty principle in the presence of quantum memory. *Nat. Phys.* **6**, 659 (2010). [arXiv:0909.0950](https://arxiv.org/abs/0909.0950)
46. Zhang, Y., Zhou, Q., Fang, M., Kang, G., Li, X.: Quantum-memory-assisted entropic uncertainty in two-qubit Heisenberg XYZ chain with Dzyaloshinskii–Moriya interactions and effects of intrinsic decoherence. *Quant. Inf. Proc.* **17**, 326 (2018)
47. Hill, S., Wootters, W.K.: Entanglement of a pair of quantum bits. *Phys. Rev. Lett.* **78**, 5022 (1997). [arXiv:quant-ph/9703041](https://arxiv.org/abs/quant-ph/9703041)
48. Wootters, W.K.: Entanglement of formation of an arbitrary state of two qubits. *Phys. Rev. Lett.* **80**, 2245 (1998). [arXiv:quant-ph/9709029](https://arxiv.org/abs/quant-ph/9709029)
49. Rigolin, G.: Thermal entanglement in the two-qubit Heisenberg XYZ model. *Int. J. Quant. Inf.* **2**, 393 (2004). [arXiv:quant-ph/0311185](https://arxiv.org/abs/quant-ph/0311185)
50. Li, D.C., Cao, Z.L.: Effect of different Dzyaloshinskii–Moriya interactions on entanglement in the Heisenberg XYZ chain. *Int. J. Quant. Inf.* **7**, 547 (2009). [arXiv:0807.1457](https://arxiv.org/abs/0807.1457)
51. Brodutch, A., Terno, D.R.: Quantum discord, local operation, and Maxwell’s demons. *Phys. Rev. A* **81**, 062103 (2010). [arXiv:1002.4913](https://arxiv.org/abs/1002.4913)
52. Modi, K., Brodutch, A., Cable, H., Paterek, T., Vedral, V.: The classical-quantum boundary for correlations: discord and related measures. [arXiv:1112.6238](https://arxiv.org/abs/1112.6238)
53. Chen, Q., Zhang, C., Yu, S., Yi, X.X., Oh, C.H.: Quantum discord of two-qubit X-states. *Phys. Rev. A* **84**, 042313 (2011). [arXiv:1102.0181](https://arxiv.org/abs/1102.0181)
54. Wang, C.Z., Li, C.X., Nie, L.Y., Li, J.F.: Classical correlation and quantum discord mediated by cavity in two coupled qubits. *J. Phys. B: Atom. Mol. Opt. Phys.* **44**, 015503 (2011)
55. Coffman, V., Kundu, J., Wootters, W.K.: Distributed entanglement. *Phys. Rev.* **A61**, 052306 (2000). [arXiv:quant-ph/9907047](https://arxiv.org/abs/quant-ph/9907047)

56. Ou, Y.U., Fan, H.: Monogamy Inequality in terms of negativity for three-qubit states. *Phys. Rev.* **A75**, 062308 (2007). [arXiv:quant-ph/0702127](https://arxiv.org/abs/quant-ph/0702127)
57. Feynman, R.P., Hibbs, A.R.: *Quantum Mechanics and Path Integrals*. McGraw-Hill, New York (1965)
58. Bennett, C.H., DiVincenzo, D.P., Smolin, J.A., Wootters, W.K.: Mixed-state entanglement and quantum error correction. *Phys. Rev.* **A54**, 3824 (1996). [arXiv:quant-ph/9604024](https://arxiv.org/abs/quant-ph/9604024)
59. Uhlmann, A.: Fidelity and concurrence of conjugate states. *Phys. Rev. A* **62**, 032307 (2000). [arXiv:quant-ph/9909060](https://arxiv.org/abs/quant-ph/9909060)

Publisher's Note Springer Nature remains neutral with regard to jurisdictional claims in published maps and institutional affiliations.